in *Computers and Structures*.

[2]Hung, N. D. and de Saxce, G., "Frictionless Contact of Elastic Bodies by Finite Element Method and Mathematical Programming Technique," *Computers and Structures*, Vol. 11, 1980, pp. 55-67.

[3]Webster, W. D. Jr. and Davis, R. L., "Development of a Friction Element for Metal Forming Analysis," *Journal of Engineering for Industry, Transactions of ASME Series B*, Vol. 104, Aug. 1982, pp. 253-256.

[4]Morris, A. J., *Foundations of Structural Optimization: A Unified Approach*, John Wiley & Sons, New York, 1982, pp. 335-358.

[5]Bathe, K. J., "ADINA—A Finite Element Program for Automatic Dynamic Incremental Nonlinear Analysis," Rept. 82448-1, Acoustic and Vibration Laboratory, Department of Mechanical Engineering, Massachusetts Insitute of Technology, Cambridge, 1975, pp. 226-228.

Transient Heat-Transfer Analysis of a Conical Cathode of an MPD Arcjet

R. C. Mehta*
Vikram Sarabhai Space Centre, Trivandrum, India

Nomenclature

A,B,C,D	= coefficients of square temperature matrix
Bi	= Biot number, hL/k
h	= heat-transfer coefficient
I	= applied current
k	= thermal conductivity
L	= cathode length
Qs	= heat transfer to cathode root
r	= cathode radius
r_o	= cathode tip radius
T	= local temperature of cathode at x
T_s	= cathode temperature at $x=0$
T_∞	= surrounding temperature
t	= nondimensional time, $\kappa\tau/L^2$
Δt	= computing time
x	= space coordinate
X	= nondimensional length, x/L
X_1	= nondimensional conical length of cathode, L_1/L
Δx	= node thickness
α	= semicone angle
ϵ	= emissivity
θ	= nondimensional temperature, T/T_s
ρ	= electrical resistivity
κ	= thermal diffusivity
σ	= Stefan-Boltzmann constant

Subscripts

i,o,R	= node identifiers
n	= designated the point $(t+\Delta t)$
$n+\frac{1}{2}$	= intermediate time level

Introduction

MOST magnetoplasmadynamic (MPD) thrusters operate at large discharge currents and low mass flow rates in order to obtain high specific impulse and thrust efficiency.[1] It is required that the cathode be operated with high temperatures at the cathode root to allow the emission of electrons with a moderate electric field while suffering minimum material loss. But severe surface erosion at the cathode tip has been observed experimentally[2,3] in transient operating conditions. In such situation, a knowledge of the temperature distribution along the cathode is essential for the thermal design of the cathode configuration. In general, 2% thoriated tungsten electrode with a semi-cone angle of 15-30 deg is employed in plasma torches and MPD arc devices.[4] A literature survey shows that transient heat-transfer analysis of the conical shape cathode has not been considered.

This Note reports a two-time level implicit scheme for the numerical solution of the nonlinear transient energy equation. As will be shown, the scheme is simple, straightforward, and unconditionally stable and convergent.

Analysis

Consider a one-dimensional cathode of conical shape with constant thermophysical properties. The configuration is as shown in Fig. 1. The nondimensional transient equation with combined conduction, ohmic heating, radiation, and convection can be written as

$$\frac{\partial^2\theta}{\partial X^2}+\frac{2\tan\alpha}{(X\tan\alpha+r_o/L)}\frac{\partial\theta}{\partial X}+\frac{I^2\rho}{kT_s[\pi(X\tan\alpha+r_o/L)]^2}-\frac{2\epsilon\sigma LT_s^3\tan\alpha}{k(X\tan\alpha+r_o/L)}\left[\theta^4-\left(\frac{T_\infty}{T_s}\right)^4\right]-\frac{2Bi\tan\alpha}{(X\tan\alpha+r_o/L)}\left[\theta-\left(\frac{T_\infty}{T_s}\right)\right]=\frac{\partial\theta}{\partial t},\quad 0<X\le X_1 \tag{1}$$

$$\frac{\partial^2\theta}{\partial X^2}+\frac{I^2\rho}{kT_s(\pi r/L)^2}-\frac{2\epsilon\sigma L^2T_s^3}{kr}\left[\theta^4-\left(\frac{T_\infty}{T_s}\right)^4\right]-\frac{2LBi}{r}\left[\theta-\left(\frac{T_\infty}{T_s}\right)\right]=\frac{\partial\theta}{\partial t},\quad X_1<X<1 \tag{2}$$

with the initial and boundary conditions

$$\theta(X,0)=T_o/T_s,\ \text{for all } X \tag{3a}$$

$$\theta(0,t)=1,\quad t>0 \tag{3b}$$

$$\frac{\partial\theta(1,t)}{\partial X}=0,\quad t>0 \tag{3c}$$

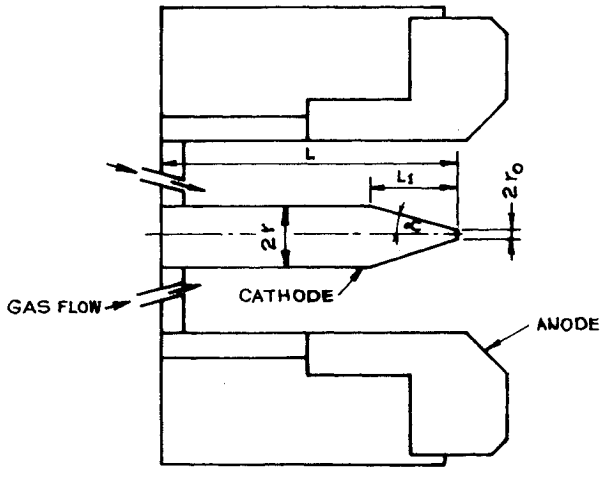

Fig. 1 Quasisteady MPD arcjet.

Received Aug. 23, 1984; revision received Jan. 14, 1985.

*Engineer, Aerodynamics Division.

Writing Eq. (1) in Crank-Nicholson, two-time level implicit form at the general node i, we can readily obtain the governing equation in a tridiagonal system of equations of the form

$$A_i\theta_{i-1,n}+B_i\theta_{i,n}+C_i\theta_{i+1,n}=D_i,\quad 2\le i\le R-1 \tag{4}$$

The coefficients may be readily obtained in the conical region for $2<i<j$ as

$$A_i=1-\frac{S(\Delta X)}{2}$$

$$B_i=-2-N_{11}(\Delta X)^2\theta_{i,n+1/2}^3-N_{12}(\Delta X)^2-\frac{2(\Delta X)^2}{\Delta t}$$

$$C_i=1+\frac{S(\Delta X)}{2}$$

$$D_i=-\left[1-\frac{S(\Delta X)}{2}\right]\theta_{i-1,n-1}-\left[1+\frac{S(\Delta X)}{2}\right]\theta_{i+1,n-1}$$
$$+\left[2+N_{11}(\Delta X)^2\theta_{i,n+1/2}^3+N_{12}(\Delta X)^2-\frac{2(\Delta X)^2}{\Delta t}\right]\theta_{i,n-1}$$
$$-2(\Delta X)^2\left[N_{11}\left(\frac{T_\infty}{T_s}\right)^4+N_{12}\left(\frac{T_\infty}{T_s}\right)+N_{13}\right]$$

and in the cylindrical region for $j<i\le R-1$ as

$$A_i=1$$

$$B_i=-2-N_{21}(\Delta X)^2\theta_{i,n+1/2}^3-N_{22}(\Delta X)^2-\frac{2(\Delta X)^2}{\Delta t}$$

$$C_i=1$$

$$D_i=-\theta_{i-1,n-1}-\theta_{i+1,n-1}$$
$$+\left[2+N_{21}(\Delta X)^2\theta_{i,n+1/2}^3+N_{22}(\Delta X)^2-\frac{2(\Delta X)^2}{\Delta t}\right]\theta_{i,n-1}$$
$$-2(\Delta X)^2\left[N_{21}\left(\frac{T_\infty}{T_s}\right)^4+N_{22}\left(\frac{T_\infty}{T_s}\right)+N_{23}\right]$$

where

$$S=\frac{2\tan\alpha}{(i-1)\Delta X\tan\alpha+r_o/L}$$

$$N_{11}=\frac{2\epsilon\sigma LT_s^3\tan\alpha}{k[(i-1)\Delta X\tan\alpha+r_o/L]}$$

$$N_{12}=\frac{2Bi\tan\alpha}{k[(i-1)\Delta X\tan\alpha+r_o/L]}$$

$$N_{13}=\frac{I^2\rho}{kT_s\{\pi[(i-1)\Delta X\tan\alpha+r_o/L]\}^2}$$

$$N_{21}=\frac{2\epsilon\sigma T_s^3L^2}{kr},\quad N_{22}=\frac{2LBi}{r},\quad N_{23}=\frac{I^2\rho}{kT_s(\pi r/L)^2}$$

The constants S, N_{11}, N_{12}, and N_{13} apply to the conical region and N_{21}, N_{22}, and N_{23} to the cylindrical region. The values of ΔX are defined as $2X_1/R$ and $2(1-X_1)/R$ in the conical and cylindrical regions, respectively, and the value of j is equal to $R/2$, where R is the total number of increments in complete intervals between 0 and 1.

The temperatures at the intermediate time $n+1/2$ can be evaluated by Taylor's forward projection method, which leads[5] to

$$\theta_{i,n+1/2}=\theta_{i,n}+\frac{\Delta t}{2(\Delta X)^2}\left\{\left[1-\frac{S(\Delta X)}{2}\right]\theta_{i-1,n}\right.$$
$$+\left[1+\frac{S(\Delta X)}{2}\right]\theta_{i+1,n}$$
$$\left.-[2+N_{11}(\Delta X)^2\theta_{i,n}^3+N_{12}(\Delta X)^2]\theta_{i,n}\right\}$$
$$+\frac{\Delta t}{2}\left[N_{11}\left(\frac{T_\infty}{T_s}\right)^4+N_{12}\left(\frac{T_\infty}{T_s}\right)+N_{13}\right],\quad 2\le i<j \tag{5a}$$

and for $j<i\le R-1$

$$\theta_{i,n+1/2}=\theta_{i,n}+\frac{\Delta t}{2(\Delta X)^2}\{\theta_{i-1,n}+\theta_{i+1,n}$$
$$-[2+N_{21}(\Delta X)^2\theta_{i,n}^3+N_{22}(\Delta X)^2]\theta_{i,n}\}$$
$$+\frac{\Delta t}{2}\left[N_{21}\left(\frac{T_\infty}{T_s}\right)^4+N_{22}\left(\frac{T_\infty}{T_s}\right)+N_{23}\right] \tag{5b}$$

At the interface ($i=j$) of the conical and the cylindrical sections of the cathode, the coefficients of the square temperature matrix are calculated by satisfying the temperature and heat flux continuity conditions.

The above forward projection scheme has less stringent restriction on the time-step size for stability and converges more rapidly as compared to backward projection method.[5]

The finite difference analog at $i=1$ can be obtained using Eq. (3b) as

$$\left[-2-N_{11}(\Delta X)^2\theta_{1,n+1/2}^3-N_{12}(\Delta X)^2-\frac{2(\Delta X)^2}{\Delta t}\right]\theta_{1,n}$$
$$+\left[1+\frac{S(\Delta X)}{2}\right]\theta_{2,n}=-\left[1+\frac{S(\Delta X)}{2}\right]\theta_{2,n-1}$$
$$+\left[2+N_{11}(\Delta X)^2\theta_{1,n+1/2}^3+N_{12}(\Delta X)^2-\frac{2(\Delta X)^2}{\Delta t}\right]\theta_{1,n-1}$$
$$-2(\Delta X)^2\left[N_{11}\left(\frac{T_\infty}{T_s}\right)^4+N_{12}\left(\frac{T_\infty}{T_s}\right)+N_{13}\right]$$
$$-2\left[1-\frac{S(\Delta X)}{2}\right] \tag{6a}$$

with

$$\theta_{1,n+1/2}=\theta_{1,n}+\frac{\Delta t}{2(\Delta X)^2}\left\{\left[1-\frac{S(\Delta X)}{2}\right]+\left[1+\frac{S(\Delta X)}{2}\right]\theta_{2,n}\right.$$
$$\left.-[2+N_{11}(\Delta X)^2\theta_{1,n}^3+N_{12}(\Delta X)^2]\theta_{1,n}\right\}$$
$$+\frac{\Delta t}{2}\left[N_{11}\left(\frac{T_\infty}{T_s}\right)^4+N_{12}\left(\frac{T_\infty}{T_s}\right)+N_{13}\right] \tag{6b}$$

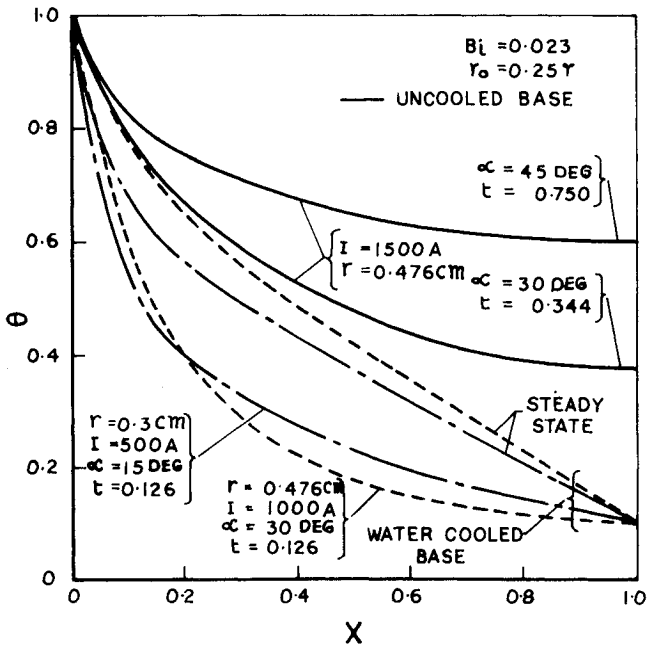

Fig. 2 Cathode temperature profiles.

Using Eq. (3c), the finite difference analog at $i=R$ is

$$2\theta_{R-1,n}+\left[-2-N_{21}(\Delta X)^2\theta^3_{R,n+\frac{1}{2}}-N_{22}(\Delta X)^2-\frac{2(\Delta X)^2}{\Delta t}\right]\theta_{R,n}=-2\theta_{R-1,n-1}+\left[2+N_{21}(\Delta X)^2\theta^3_{R,n+\frac{1}{2}}+N_{22}(\Delta X)^2-\frac{2(\Delta X)^2}{\Delta t}\right]\theta_{R,n-1}-2(\Delta X)^2\left[N_{21}\left(\frac{T_\infty}{T_s}\right)^4+N_{22}\left(\frac{T_\infty}{T_s}\right)+N_{23}\right] \tag{7a}$$

with

$$\theta_{R,n+\frac{1}{2}}=\theta_{R,n}+\frac{\Delta t}{2(\Delta X)^2}\{2\theta_{R-1,n}-[2+N_{21}(\Delta X)^2\theta^3_{R,n}+N_{22}(\Delta X)^2]\theta_{R,n}\}+\frac{\Delta t}{2}\left[N_{21}\left(\frac{T_\infty}{T_s}\right)^4+N_{22}\left(\frac{T_\infty}{T_s}\right)+N_{23}\right] \tag{7b}$$

From a Taylor's series expansion the local order of accuracy can be shown to be $\epsilon_i^{n+\frac{1}{2}}=\mathcal{O}[(\Delta X)^2+(\Delta t)^2]$, which is the same as the linear case. The system of difference equations will be stable and converge according to Refs. 5 and 6.

The tridiagonal system of Eqs. (4-6) can be solved using Thomas algorithm.[5] A FORTRAN computer program has been prepared for the computation of temperature distribution along the cathode. The computations have been performed on Cyber 170/730 digital computer for an applied current strength of 500-2000 A, cathode length of 2.54 cm, radius of 0.3 and 0.476 cm, semicone angle of 15-45 deg, and heat-transfer coefficient[4] equal to 100 W/m^2·K. For computational purposes, $T_s=3000$ K has been selected, which is below the melting point of tungsten.[7] T_o and T_∞ are taken as 300 and 450 K, respectively. The material properties[4] taken are $\epsilon=0.4$, $k=110$ W/m·K, and $\rho=55\times10^{-8}$ Ω·m.

Fine and coarse grid spacing are used in the conical and cylindrical regions of the cathode, respectively. Twenty grid points and a time interval of 0.313E−03 are taken for computational purposes. Thus, the dimensionless time step $[(\Delta t)/(\Delta X)^2]$ has different values in different regions of the cathode.

Results and Discussions

Temperature distributions along the cathode for various values of electric current and geometrical configuration are depicted in Fig. 2. In order to obtain accuracy and convergence of the finite difference solution, temperature distribution along the cathode for $r=0.3$ and 0.476 cm, $\alpha=15$ and 30 deg, and $I=500$ and 1000 A are computed, while keeping the other end of the cathode at temperature equal to 300 K. It can be seen that the temperature profiles reached steady state from a transient condition. The steady-state temperature profiles are compared with the numerical integration solution[4] and are found to be in good agreement. It is seen that the temperature decreases rapidly along the nose cone portion of the cathode, while in the remaining length of the cathode the temperature varies gradually. The conduction-radiation and the ohmic heating parameters have a significant influence on the temperature distribution in the conical portion of the cathode. It is important to mention here that N_{11}, N_{12}, and N_{13} are functions of the radius of the conical region, whereas N_{21}, N_{22}, and N_{23} are constant in the cylindrical region of the cathode.

Transient temperature distributions at $t=0.344$ and 0.75 are shown for uncooled cathode base at $\alpha=30$ and 45 deg, respectively, while keeping the other variables unchanged. For a small increase in time, heat transfer Qs to the cathode reaches a zero value and the temperature at the cathode root exceeds the melting point of tungsten. This is attributed to excessive joule heating near the vicinity of the cathode tip. It can also be seen that the larger semicone angle of the cathode can withstand melting for a longer time compared to a smaller semicone angle.

The present analysis is useful in finding the safe operating time limit for a plasma torch in case of a coolant failure to a cathode. An extension of this analysis makes it possible to predict the thermal response of a conical cathode of a MPD arcjet when it operates intermittently.

References

[1]Turchi, P. J. and John, R. G., "Cathode Region of a Quasi-steady MPD Arc Jet," *AIAA Journal*, Vol. 9, July 1971, pp. 1372-1379.

[2]Kuriki, K., Chnishi, M., and Morimoto, S., "Thrust Measurement of K III MPD Arcjet," *AIAA Journal*, Vol. 20, Oct. 1982, pp. 1414-1419.

[3]Kimura, I., Toki, K., and Tanaka, M., "Current Distribution on the Electrodes of MPD Arcjet," *AIAA Journal*, Vol. 20, July 1982, pp. 1062-1067.

[4]Mehta, R. C., "Thermal Analysis of a Conical Cathode of an MPD Arc," *AIAA Journal*, Vol. 17, Nov. 1979, pp. 1272-1274.

[5]vonRosenberg, D. U., *Methods for the Numerical Solutions of Partial Differential Equations*, Elsevier Publishing Co., New York, 1969.

[6]Mehta, R. C., "Numerical Solution of Nonlinear Inverse Heat Conduction Problem with a Radiation Boundary Condition," *International Journal of Numerical Methods in Engineering*, Vol. 20, June 1984, pp. 1057-1066.

[7]Shih, K. T., Pfender, E., and Eckert, E. R. G., "Thermal Analysis of Cathode and Anode Regimes of an MPD Arc," NASA CR 54664, Jan. 1968.